

SOLAR ENERGETIC PARTICLE EVENTS AND THE KIPLINGER EFFECT

S. W. KAHLER

Air Force Research Laboratory, RVBXS, 3550 Aberdeen Avenue, Kirtland AFB, NM 87117, USA; AFRL.RVB.PA@hanscom.af.mil

Received 2011 July 19; accepted 2011 November 28; published 2012 February 15

ABSTRACT

The Kiplinger effect is an observed association of solar energetic ($E > 10$ MeV) particle (SEP) events with a “soft–hard–harder” (SHH) spectral evolution during the extended phases of the associated solar hard ($E > 30$ keV) X-ray (HXR) flares. Besides its possible use as a space weather predictor of SEP events, the Kiplinger effect has been interpreted as evidence of SEP production in the flare site itself, contradicting the widely accepted view that particles of large SEP events are predominately or entirely accelerated in shocks driven by coronal mass ejections (CMEs). We review earlier work to develop flare soft X-ray (SXR) and HXR spectra as SEP event forecast tools and then examine recent *Reuven Ramaty High-Energy Solar Spectroscopic Imager (RHESSI)* evidence supporting the association of SHH HXR flares with large SEP events. We point out that ad hoc prediction criteria using the CME widths and SXR flare durations of associated *RHESSI* hard X-ray bursts (HXBs) can yield results comparable to those of the SHH prediction criteria. An examination of the *RHESSI* dynamic plots reveals several ambiguities in the determination of whether and when the SHH criteria are fulfilled, which must be quantified and applied consistently before an SHH-based predictive tool can be made. A comparative HXR spectral study beginning with the large population of relatively smaller SEP events has yet to be done, and we argue that those events will not be so well predicted by the SHH criteria. SHH HXR flares and CMEs are both components of large eruptive flare events, which accounts for the good connection of the SHH HXR flares with SEP events.

Key words: acceleration of particles – Sun: coronal mass ejections (CMEs) – Sun: flares – Sun: particle emission – Sun: X-rays, gamma rays

Online-only material: color figures

1. INTRODUCTION

Solar flare hard ($E > 30$ keV) X-ray bursts (HXBs) can broadly be classified as impulsive or gradual. An early review of the two burst categories by Dennis (1988) made the following distinctions. Impulsive HXBs (IHXBs) are characterized by short spikes with variability on timescales of seconds, low source altitudes of ≤ 2500 km, and evolution with a soft–hard–soft (SHS) spectral behavior. The gradual HXBs (GHXBs) are found to be gradually varying on timescales of minutes and sometimes lasting 30 minutes or longer; located at high (4×10^4 km) altitudes; and evolving with a soft–hard–harder (SHH) spectral behavior above ~ 50 keV. GHXBs are much less frequent, perhaps $\leq 20\%$ of the IHXBs (Kosugi et al. 1988) and tend to be associated with the most intense flares. An early survey by Cliver et al. (1986) of ten GHXBs found them to occur in the late phases of major flares and to be associated with coronal mass ejections (CMEs) and post-flare loop systems. They proposed that the radiating electrons were trapped in the post-flare loops as illustrated by a popular schematic reproduced as in Figure 1.

A connection between interplanetary solar energetic ($E > 10$ MeV) particle (SEP) events and SHH HXBs was established by Kiplinger (1995) on the basis of two studies to match SEP events with HXBs observed with the Hard X-ray Burst Spectrometer (HXRBS) on the *Solar Maximum Mission (SMM)* satellite. A goal of those studies was to use observational associations to “forecast” or “predict” the presence or the absence of subsequent HXB-associated SEP events. In this spirit we use the terms forecasts, predictions, and associations interchangeably. An unsuccessful, or incorrect, prediction is either false, when a predicted SEP event does not occur, or a miss, when an SEP event occurs despite a prediction of no event.

The flare SHH criteria adopted from these studies provided successful predictions of 22 of 23 NOAA Space Environment Services Center (now Space Weather Prediction Center) SEP events, defined to have peak flux thresholds of $F_p > 10$ protons $(\text{cm}^2 \text{ s sr})^{-1}$ for $E > 10$ MeV, known as 10 pfu. Kiplinger’s (1995) criteria further correctly forecast no associated NOAA SEP event for 700 of 708 non-SHH HXBs. The implications of this remarkable forecasting success rate of 96% and 99% for predicting and rejecting, respectively, SEP events have been widely noted for both space weather forecasting and the physics of SEP acceleration sources. Subsequent observations of the large 2005 January HXBs (Saldanha et al. 2008) and a survey of HXBs (Grayson et al. 2009) with the *Reuven Ramaty High-Energy Solar Spectroscopic Imager (RHESSI)* provided new support for the SEP connection with SHH XRBs. Hudson (2011) has recently enhanced the status of this result with the term “Kiplinger effect,” which we follow here.

The consensus view of large gradual SEP events is that the SEPs are accelerated in shocks driven by fast and wide CMEs (Reames 1999; Kahler 2005; Cliver 2009). However, an alternative view based on elemental abundance variations among gradual SEP events (Cane et al. 2006, 2010) or on temporal correlations of flare soft X-ray (SXR; Firoz et al. 2011) or impulsive hard X-ray (Aschwanden 2012) profiles with those of ground-level events (GLEs) favors the flare process as an important source of those SEPs. Kocharov et al. (2010, 2011) propose that SEP acceleration occurs with coronal reconnection and turbulence in closed flare structures, followed by particle release during the associated CME. The inferred solar injection of GeV particles at the time of the flare impulsive phase in the 2005 January 20 GLE suggested to some (Simnett 2006; Kuznetsov et al. 2008) the flare as the only significant GeV SEP source. Two apparent pulses of GeV particles in the

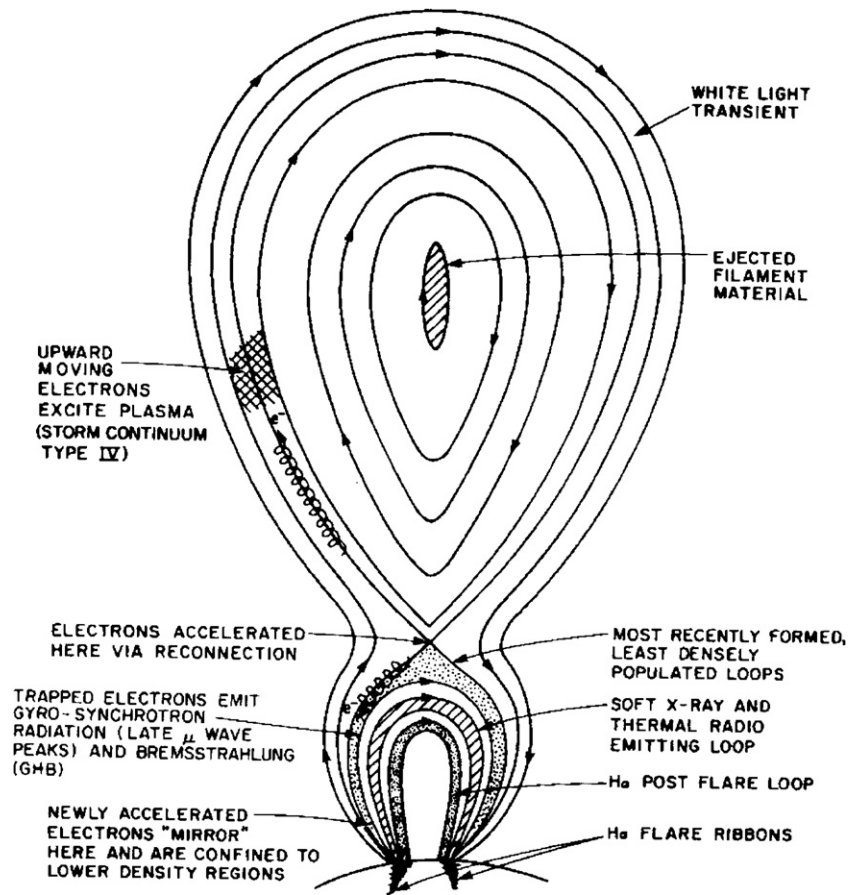


Figure 1. Geometry of an eruptive event proposed by Cliver et al. (1986) showing the region of energetic trapped electrons giving rise to the GHXB.

intensity profile of that and other GLE events spurred the interpretation of an initial flare-produced GeV component with a hard energy spectrum followed by a second CME shock-produced component with a softer spectrum (Grechnev et al. 2008; McCracken et al. 2008; Masson et al. 2009). Another view (Vashenyuk et al. 2009; Miroschnichenko et al. 2009; Perez-Peraza et al. 2009) holds that the CME shock contributes only non-relativistic SEPs, so that both phases of GLE events are attributed to flare processes.

In the context of a flare source for SEPs the Kiplinger effect could be a manifestation of the flare acceleration mechanism giving rise to the population of gradual SEP events. Kiplinger (1995) pointed to observed correlations of the logs of the SEP event F_p with the logs of the SHH hardening timescales T_{shh} and with the logs of the hard X-ray flare durations as evidence that the HXBs and SEP events share common physical mechanisms of high-energy particle acceleration that can occur over a wide range of timescales. In his view the SHH source region was larger than the impulsive flare and smaller than the associated CME regions, thereby implicitly excluding CME shocks as the primary SEP sources.

The Kiplinger effect is consistent with the concept of flare sources for interplanetary SEP events and therefore at odds with the conventional CME-shock source interpretation. The recent supporting work makes it imperative to examine critically the characteristics of the SHH signatures and the connections between SHH XRBs and gradual SEP events. In addition, comparisons of the signatures of both flares and CMEs in those SEP events are needed for context. The goal of this work is to compare the statistics of the Kiplinger effect with those of other

predictive signatures of SEP events and to address the apparent contradiction of the Kiplinger effect with the paradigm of shock acceleration. We first review in Section 2 the work connecting both SXR flares and SHH XRBs to SEP events. The goal here is to provide a comprehensive summary of the earlier and recent work, compiling the various reported association statistics of SEP events in common tables. The selection criteria of each data set are given to allow easy comparisons among the studies and to assess their strengths and limitations.

In Section 3, we discuss the two recent studies with *RHESSI* XRB observations that have brought new attention to the Kiplinger effect and point out the important roles of SXR flares and fast CMEs in those observations. In Section 4, several poorly defined characteristics of the SHH criteria that must be clearly quantified to develop a useful predictive tool for SEP events are reviewed. We address in Section 5 the basic question of how CMEs, flare HXBs, and SEP events are related and summarize the results in Section 6. The basic conclusion here is that the SHH criteria may work well to forecast NOAA SEP events only because the energetic CMEs that drive the shocks to produce SEPs are also closely coupled to eruptive flares with SHH HXBs.

2. REVIEW OF SXR AND HXB FLARE/SEP EVENT RELATIONSHIPS

2.1. Relating Low-temperature SXR Flares to HXBs and SEP Events

A tortuous history of studies connects SEP events with associated SXR flares, SHH HXBs, and CMEs. Separating the various connections among these phenomena is important for

Table 1
Combined Contingency Table for NOAA SEP Event Studies

Study	Criterion	SEP Event Observed	No SEP Event Observed
A (Garcia 1994) ^a	GHXB associated	16	1
	GHXB not associated	0	115
B (Kiplinger 1995) ^b	HXB SHH	4	1
	HXB no SHH	0	188
C (Kiplinger 1995) ^c	HXB SHH	10	5
	HXB no SHH	1	136
D (Kiplinger 1995) ^d	HXB SHH	22	8
	HXB no SHH	1	700
E (Garcia 2004b) ^e	HXB $\gamma < 4$ met	14	3
	HXB $\gamma < 4$ not met	2	87
F (Grayson et al. 2009) ^f	HXB SHH	5	5
	HXB no SHH	0	21

Notes.

^a All GHXBs with $\geq M5$ flares west of $E60^\circ$ and all NOAA SEP events.

^b All HXRBS/*SMM* HXBs with 800–5000 photons s^{-1} and all NOAA SEP events. $T_{shh} > 70$ s required for NOAA SEP event prediction, and prediction of no NOAA SEP event if flare $\leq X1.0$ and location east of $E40^\circ$.

^c All HXRBS/*SMM* HXBs with ≥ 5000 photons s^{-1} reclassified from part B to include only NOAA SEP events. Prediction criteria of part C also required.

^d Weighted totals of all HXRBS/*SMM* HXBs with ≥ 800 photons s^{-1} and only NOAA SEP events. $T_{shh} > 70$ s required for NOAA SEP event prediction, and prediction of no NOAA SEP event if flare $\leq X1.0$ and location east of $E40^\circ$.

^e 106 HXRBS/*MTI* HXBs with $\gamma < 4$ for ≥ 3 minutes and NOAA SEP events.

^f 31 *RHESSI* well-connected ($W30^\circ$ – $W90^\circ$) full-coverage HXBs with SHH evolution satisfying the Kiplinger criteria and associated NOAA SEP events. Three SHH events in which $T_{shh} < 70$ s are included in the 21 events with no SHH and no NOAA SEP event.

understanding the relationship between the SHH HXBs and SEP events in a broader context and to determine the basic physics of SEP production. The details of this review section, however, are cumbersome and are not required to understand the discussion in subsequent sections. We start with Garcia & McIntosh (1992), who calculated SXR flare temperatures with observations from the 0.5–3 and 1–8 Å broad-band detectors on the *Geostationary Operational Environmental Satellite* (*GOES*) satellites and found that the 54 high-temperature ($T > 25$ MK) flares observed among 710 large SXR flares were preferentially associated with IHXBs rather than with GHXBs. For flares smaller than X class, the GHXBs were preferentially associated with cooler than average SXR flares. In extending the statistical studies to SEP events, Garcia (1994, 2004a) showed that in the flare size range M1 to X2 the *GOES* flares associated with NOAA SEP events were significantly cooler than the “normal” flares without SEP events. A second comparison showed that lower temperatures and longer durations of SXR flares statistically favored associations with both GHXBs and SEP events over IHXBs and non-SEP events, respectively. Nonast et al. (1982) and Kubo & Akioka (2004) found large SXR flare fluences and long decay times or durations to be good signatures for large SEP events, indicating the importance of long flare timescales rather than peak flare fluxes in the SEP associations. These studies therefore established a tendency for correlations of both SEP events and GHXBs with longer and

Table 2
Combined Contingency Table for Studies with All SEP Events

Study	Criterion	SEP Event Observed	No SEP Event Observed
A (Kiplinger 1995) ^a	HXB SHH	18	6
	HXB no SHH	4	124
B (Grayson et al. 2009) ^b	HXB SHH	13	5
	HXB no SHH	1	18
C (This study) ^c	GOES D > 25 minutes	11	2
	GOES D < 25 minutes	3	21
D (This study) ^d	CME W > 120°	13	2
	CME W $\leq 120^\circ$	0	14

Notes.

^a All HXRBS/*SMM* HXBs with ≥ 5000 photons s^{-1} and all Fp > 0.1 pfu SEP events associated with those HXBs.

^b 37 *RHESSI* well-connected ($W30^\circ$ – $W90^\circ$) full-coverage HXBs with SHH evolution at any timescale and associated SEP events ≥ 0.1 pfu. See the text for two changes from the original Table 2 of Grayson et al. (2009).

^c 37 associated *GOES* SXR from Table 2 of Grayson et al. (2009). Criterion for SEP event is *GOES* duration D > 25 minutes.

^d 29 associated LASCOS CMEs from Table 2 of Grayson et al. (2009). Criterion for SEP event is CME W > 120° .

cooler SXR flares. The lower SXR flare temperatures were attributed to the higher altitudes and lower particle densities of the coronal source regions, consistent with the concept of Cliver et al. (1986) for GHXBs.

Directly comparing all 16 NOAA SEP events with adequate associated *SMM* observations and GHXBs in a two-year period, Garcia (1994) found a very close association: NOAA SEP events almost always followed large GHXBs, and conversely, sufficiently well connected (west of $E60^\circ$) GHXBs preceded NOAA SEP events. Subject to several important selection criteria, his SEP–GHXB contingency table contained 131 correct associations and only one incorrect association, as shown in part A of Table 1. We will use Tables 1 and 2 as the basis for direct comparisons of various SEP association contingency tables to be discussed below.

2.2. The Kiplinger (1995) Studies: SHH XRBs and SEP Events

As pointed out in Sections 1 and 2.1, the GHXBs and IHXBs are generally characterized by SHH and SHS spectral behavior, respectively, and SEP events are well associated with the GHXBs. However, SHH behavior can be found through individual peaks of HXBs as well as during HXB decay phases (Dennis 1988). The prominent work of Kiplinger (1995) changed the focus of SEP event associations from GHXBs to SHH HXBs, which could be either GHXBs or IHXBs. He examined 152 HXRBS/*SMM* HXBs selected for complete event observations, a peak HXB counting rate $R_p > 5000$ counts s^{-1} , and an unambiguous determination of whether an $E > 10$ MeV SEP event of Fp > 0.1 pfu was associated with the HXB. Those HXBs were examined for SHH behavior, regardless of the timescales of that behavior. Spectral fits over the ~ 30 –500 keV range were done with variable time intervals with a minimum of 400 photons. SHH behavior was found through individual peaks (denoted as HPs) or during decays (denoted as HDs) of some HXBs. The good association between the 24 SHH HXBs and 22 SEP events of the 152 HXBs is shown in part A of

Table 2. Three of the six SHH HXB events east of E40° were not associated with SEP events, again showing the importance of magnetic connection effects. Note that $F_p > 0.1$ pfu SEP events not associated with the selected 152 HXBs were not a part of that study.

Kiplinger's (1995) second, reverse study was limited to NOAA SEP events and expanded to all HXRBS flares with peak counting rates in the lower range of $800 \text{ counts s}^{-1} < R_p < 5000 \text{ counts s}^{-1}$. Only every third qualifying flare of the HXRBS catalog was used to get a manageable number of 193 HXBs. Based on his first study, two new prediction criteria for NOAA SEP events were introduced: $T_{\text{shh}} > 70$ s for the longest FWHM of hardening peaks required for event prediction; and prediction of no event if the *GOES* peak $\leq X1.0$ and the event is east of E40°. This scheme correctly predicted four NOAA SEP events and 188 non-events. There was only one false prediction and no missed event (part B of Table 1). The next step was to combine the two studies into a single algorithm to predict NOAA SEP events from SHH HXBs. First, the results of the study with the 152 $R_p > 5000 \text{ counts s}^{-1}$ HXBs were reclassified to consider only NOAA SEP events and to include the two new prediction criteria. That revised contingency table is given in part C of Table 1. Assuming that all the HXRBS/*SMM* HXBs of $800 \text{ counts s}^{-1} < R_p < 5000 \text{ counts s}^{-1}$ would have had the same statistics as the one-third sample of the second study (part B of Table 1), multiplying the results of those HXBs by 3, and adding them to the reclassified events of part C of Table 1 yields the results for 731 HXBs shown in part D of Table 1 and introduced in Section 1.

Several limitations of this work should be noted here. The study is not symmetrical in that all HXRBS/*SMM* HXBs with $\geq 800 \text{ counts s}^{-1}$ were used, but no inverse study based on all observed SEP events above some lower threshold was done. The statistics are also strongly dominated by the 700 non-SHH HXBs with no observed NOAA SEP events. Since 80% of those 700 HXBs are relatively small HXRBS ($< 5000 \text{ counts s}^{-1}$) HXBs, which do not forecast the largest SEP events, the predictive value for those events is not high. In addition, the 22 correctly predicted SEP events are heavily weighted by the $3 \times$ scaling of the four actually observed events in the smaller HXB counting rate study. Thus, more than half of the 22 events are based on a number with a 50% uncertainty, and only 14 events were actually observed. Finally, the familiar 96% success rate (22 of 23 associations) applies only to observed NOAA SEP events and does not include the eight false predictions associated with SHH HXBs.

2.3. The XRB Spectral Index and a Success Criterion

An independent SEP-event study by Garcia (2004b) comparing 106 HXBs in the range 13–219 keV with the HXRS experiment on the *Multispectral Thermal Imaging (MTI)* satellite came up with less dynamic HXB spectral forecasting requirement. Rather than the SHH criteria of Kiplinger (1995), Garcia (2004b) required the HXR spectral index $\gamma < 4$ over ≥ 3 minutes. The statistics of his study to forecast NOAA SEP events are shown in part E of Table 1 (the table event total is 106, although he reported 107). If we omit the large numbers of successful predictions of no SEP events and define a prediction success metric M_{scs} as the ratio of correct to incorrect (false and missed) SEP event predictions, then his M_{scs} of 14/5, not using the SHH criteria, compares favorably with the Kiplinger (1995) 22/9 result given in part D of Table 1.

2.4. RHESSI SHH XRBs and SEP Events

The *RHESSI* mission has provided an opportunity for further testing of the Kiplinger effect. Saldanha et al. (2008) looked at the ~ 50 – 200 keV X-ray profiles of five large HXBs in 2005 January and found that γ showed some SHH behavior in four HXBs with associated SEP events near or above the NOAA SEP threshold. The one HXB at 00:43 UT on 2005 January 15 did not show SHH behavior and was not associated with an SEP event. Thus, all five HXBs were consistent with the Kiplinger effect.

Grayson et al. (2009) extended the Saldanha et al. (2008) study to include all M and X class *RHESSI* flares of Solar Cycle 23 meeting the following conditions: (1) the flare longitude range is W30°–W90°, (2) at least partial *RHESSI* observational coverage, and (3) the presence of clear non-thermal HXR emission above background. The spectral fits were done over the range from ~ 30 – 40 keV to ~ 50 – 100 keV, depending on event size, to look for SHH behavior at any timescale. Several SEP experimental data sets were examined to search for SEP events of any intensity, generally down to a level of ~ 0.1 pfu. Of the 60 cases with unambiguous spectral behavior and determination of SEP event associations, there were 24 with full *RHESSI* flare observational coverage and 13 with partial coverage adequate to show SHH behavior. Omitted were 23 events with partial observational coverage and no observed SHH behavior. We would disagree with two of the SEP associations of their Table 2. The 2005 January 19 flare at 08:22 UT, which showed SHH behavior, should be associated with a small SEP event observed with the EPACT instrument on *Wind*, improving their statistics. On the other hand, the 2002 August 3 flare, which did not show SHH behavior, is associated with a small event observed in EPACT (see Table 2 of Kahler 2005). This shifts the total for all SEP events in their Table 1 from 12, 6, 0, and 19 to 13, 5, 1, and 18, respectively, leaving the incorrect forecast total unchanged at six of 37 events. Part B of Table 2 shows our revision of their Table 1 as the basis for comparisons below.

In comparing with the Kiplinger (1995) criteria for predictions of NOAA SEP events, Grayson et al. (2009) deleted seven cases of SEP events with high backgrounds that were not listed as separate NOAA events. Grayson et al. (2009) further added one additional NOAA SEP event and omitted three events with $T_{\text{shh}} < 70$ s. Since those omitted events would be predictive of no SEP event with the Kiplinger criteria, we have added them back and show the statistics of the 31 events in part F of Table 1. It is important to note that any SEP events not associated with the 37 observed *RHESSI* HXBs were not part of this study.

2.5. A Summary of the Statistical Studies

Several characteristics dominate the pre-*RHESSI* studies in Tables 1 and 2. The first is the large number of cases with an HXB no SHH criterion and a prediction of no SEP event. These HXR flares are generally the smallest and commonest flares, for which one would not expect a priori subsequent associated SEP events. For this reason we introduced in Section 2.3 the parameter M_{scs} as a more meaningful measure of the prediction success.

A second feature of these studies is that the two alternative HXB criteria of Garcia (1994, 2004b) yielded comparable values of M_{scs} , suggesting that the SHH criterion is simply one of several criteria that may be used to predict SEP events with some success. Not included in Table 1 are the continuous probability distributions for SEP events as a function of the flare

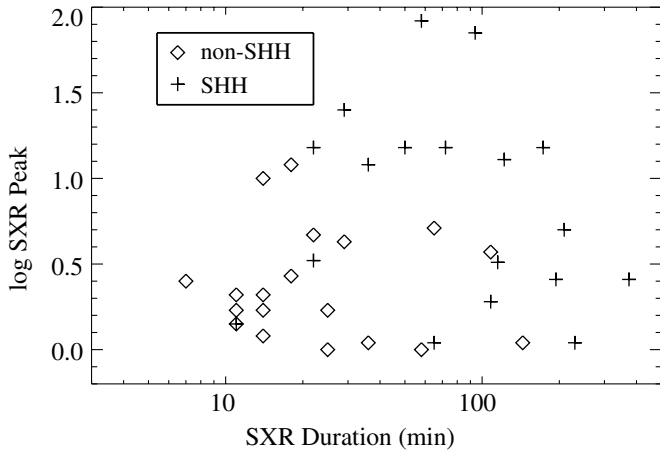


Figure 2. Plot of logs of associated SXR peak intensities vs. SXR durations for 19 non-SHH (diamonds) and 18 SHH events (circles) of the Grayson et al. (2009) study. The SXR flares of the non-SHH events are generally small and short; those of the SHH events are larger and longer. Solid symbols are SEP events; open symbols are non-SEP events.

SXR temperature (Section 2.1), but Figure 2 of Garcia (1994) suggests that criteria could have been adopted with comparable M_{scs} values. Similarly good forecasting criteria could probably also be based on SXR fluences (Kubo & Akioka 2004) or decay times (Nonnast et al. 1982). These various SXR and HXR forecasting parameters are connected in a common theme with solar eruptive flares (Cliver et al. 1986).

3. SXR FLARE AND CME PARAMETERS AS SEP PREDICTORS

3.1. Soft X-Ray Timescales as Predictive Parameters of SEP Events

In the Grayson et al. (2009) study, reviewed in Section 2.4, they examined the SXR *GOES* classes and durations of all their 18 SHH HXBs to understand better the six (revised to five events in part B of Table 2) SHH HXBs without associated SEP events. Those six events were clustered toward smaller SXR peaks and durations (their Figure 4), but were also accompanied by several of the 12 SEP-associated SXR events. They suggested that the complexities of the interplanetary magnetic field may have rendered the six non-events less well connected than for the SEP events. In Figure 2, we expand their comparison to plot the logs of the *GOES* SXR peaks against the durations for all their 37 events. We take the durations D from Table 1 of Grayson et al. (2009) and treat the 2002 August 3 and 2005 January 19 08:22 UT cases as SEP events (Section 2.4). Only three of 24 *GOES* events with short duration ($D < 25$ minutes) were associated with SEP events, and only two of the 13 long duration ($D > 25$ minutes) events were not associated with SEP events (part C of Table 2). An arbitrary choice of $D > 25$ minutes for SEP event forecasts therefore gives an $M_{scs} = 11/5$ for D that matches the $M_{scs} = 13/6$ for the SHH criterion (part B of Table 2).

The distinction between short and long SXR durations carries over to the *RHESSI* event selections. The shorter duration, smaller peak flux SXR events, which are less likely to be associated with SEP events, are also more likely to be associated with full orbital *RHESSI* coverage. Those with SEP events and longer SXR durations are more likely to require much longer observing times than afforded by the *RHESSI* data coverage. The *RHESSI* partial coverage of the latter events of the

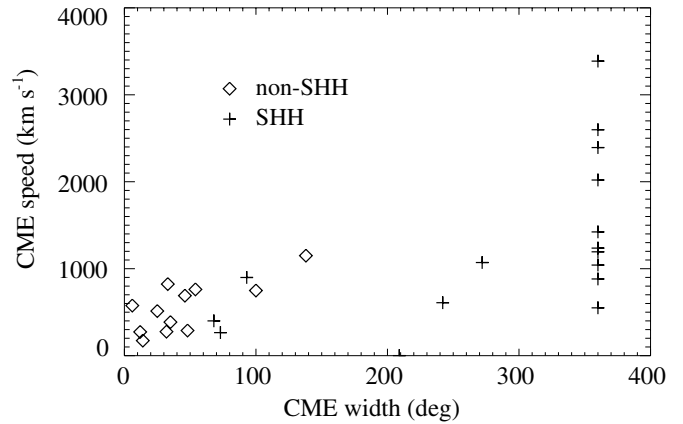


Figure 3. Plot of speeds v vs. widths W for the 29 CMEs of the Grayson et al. (2009) study. Circles indicate the 17 SHH events and diamonds the 12 non-SHH events. Solid symbols are SEP events; open symbols are non-SEP events. The dashed lines delineate the CME FW limiting criteria of 900 km s^{-1} and 60° . The log scales emphasize the distinction between the SHH and non-SHH groups. Halo ($W = 360^\circ$) CMEs are clustered at the right side.

Grayson et al. (2009) study is given as “partial” in Column 5 of their Table 1. We have examined intervals over which the spectra were calculated in the *RHESSI* HXB plots used in the Grayson et al. (2009) analysis. The median time intervals for full and partial coverage events were 5 and 19 minutes, respectively. It is perhaps not surprising that another simple ad hoc prediction criterion of *RHESSI* partial coverage for SEP events and full coverage for no SEP events also yields $M_{scs} = 11/5$, again comparable to $M_{scs} = 13/6$ for the SHH criterion.

3.2. CME Associations and SHH Flares

Grayson et al. (2009) found that most of their 38 HXBs were associated with LASCO CMEs. Two (2003 June 13 and 2004 September 19) of those HXBs occurred during LASCO data gaps. CMEs were associated with all 17 of the remaining SHH HXBs, but with only 13 of the 19 non-SHH HXBs, providing another distinction between the two HXB groups. Furthermore, Grayson et al. (2009) found a much higher average CME speed of 1342 km s^{-1} for the SHH HXBs than the 555 km s^{-1} average for the non-SHH HXBs. Here we take this comparison a step further, based on the observations of Kahler & Reames (2003) and Gopalswamy et al. (2001) that nearly all CMEs associated with SEP events and decametric–hctometric (DH) type II bursts, respectively, have widths $W > 60^\circ$. This result has led to the concept of fast ($v \geq 900 \text{ km s}^{-1}$) and wide ($W \geq 60^\circ$) (FW) CMEs as a nearly necessary condition to drive shocks (Michalek et al. 2007; Gopalswamy et al. 2008).

The CME projected speeds versus widths are plotted on log scales in Figure 3, delineating the FW regime and distinguishing the SHH from the non-SHH HXBs. The 2002 February 20 non-SHH event is not plotted because the SEP association was uncertain. The SHH-associated CMEs are much wider and in most cases are halo ($W = 360^\circ$) events. The only non-SHH FW CME is that of 2002 August 3, which was in fact a small SEP event, as discussed in Section 2.4. None of the other 11 non-SHH-associated CMEs qualified as an FW CME, and for six non-SHH HXBs there was no associated CME. Some of the SHH-associated CMEs are slower, but all are wider than the FW CME criteria.

From Figure 3, the LASCO FW CME criterion to predict SEP events gives an $M_{scs} = 10/5$. A similar exercise with only CME $v \geq 900 \text{ km s}^{-1}$ also yields $M_{scs} = 10/5$. The sole criterion

Table 3
2005 January Solar Events and SEP Production

SXR Peak (2005, UT)	GOES Class & Longitude	GOES SXR Duration ^a	LASCO CME Speed	Type II Burst Time (UT)	Peak > 10 MeV P (pfu)	HXB Spectral Evolution	Kiplinger Prediction
Jan 15 00:43	X1.2 E08°	43 minutes	No CME	None	< 0.3	SHS	No
Jan 15 06:38	M8.6 E04°	176 minutes	2049 km s ⁻¹	0555–0612	~8	NA	NA
Jan 15 23:02	X2.6 W05°	180 minutes	2861 km s ⁻¹	2224–2258	~300	SHS, then SHH	Yes
Jan 17 09:52	X3.8 W25°	137 minutes	2547 km s ⁻¹	0943–0947	~4000	SHS, then SHH	Yes
Jan 19 08:22	X1.3 W51°	122 minutes	2020 km s ⁻¹	0812–0818	~100	SHS, decay SHH	Yes
Jan 20 07:01	X7.1 W61°	90 minutes	^b 3675 km s ⁻¹	0644–0700	~1500	SHH	Yes

Notes.

^a Duration measured at 10% of peak.

^b Speed from Gopalswamy et al. (2005).

of $W > 60^\circ$ yields a higher value of $M_{scs} = 13/6$, but we can take $W > 2 \times 60^\circ = 120^\circ$ as an even better simple ad hoc SEP event predictor. Part D of Table 2 shows the contingency table for the 120° requirement for the 29 SEP events. With only two false event forecasts (2002 December 22 and 2003 May 29) the $W > 120^\circ$ criterion is better ($M_{scs} = 13/2$) than the SHH criterion of Grayson et al. (2009) for either all SEP events (13/6) or NOAA SEP events (5/5). Taking the additional six cases of no associated CMEs to be equivalent to very narrow CMEs, the 14 predictions of narrow CMEs and no SEP events is increased to 20, and only two of the 35 cases are incorrect forecasts. Thus, simple ad hoc cuts on CME v and W in this small sample can yield comparable or better results than the SHH criterion, suggesting that CME properties, and by implication shock properties, are at least as important as those of flares for SEP production.

3.3. The 2005 January HXBs

The Saldanha et al. (2008) study of *RHESSI* HXB spectra of five of the six $\geq M8.5$ GOES flares during the very active 2005 January 14–21 period found four flares with SHH and associated SEP events and one flare with no SHH and no associated SEP event, providing a recent validation of the Kiplinger effect. The six flares are listed in Table 3, where we take the flare and SEP properties from Table 1 of Saldanha et al. (2008) but correct their values of the peak proton flux for the third and fifth events. The last five events would be expected to produce SEP events from CME-driven shocks based on their associations with fast (≥ 2000 km s⁻¹) CMEs and metric type II bursts. Despite its size, the X1.2 flare on 2005 January 15 00:43 UT had no associated LASCO CME or type II burst, one of 13 such X-class flares during solar cycle 23 (Gopalswamy et al. 2009). All CMEs associated with X-class flares are visible in LASCO, although about 10% of those flares are confined and not associated with CMEs (Yashiro et al. 2005).

The January 15 X1.2 flare also had a distinctly shorter timescale than the other five large flares. The NOAA criteria for the SXR duration is defined as the interval from first monotonic increase until the flux decays to halfway between the peak flux and pre-flare background (Grayson et al. 2009). This definition stresses the flare onset phase and may not capture the decay phase well. To get a better description of the overall SXR flux profile we take the flare duration as the interval when the flux is $\geq 10\%$ of the peak flux. This definition yields a duration of 43 minutes for the X1.2 flare, much shorter than for any of the other five flares (Table 2). These events fit the general trend of higher CME associations for X-ray flares of increasing duration and fluence (Yashiro & Gopalswamy 2008).

Thus, besides the lack of an SHH signature, the January 15 flare was qualitatively different from the other 2005 January flares in showing characteristics of an impulsive, non-eruptive solar flare.

4. CAVEATS FOR DETERMINATION OF SHH SPECTRAL BEHAVIOR

4.1. SHH Burst Sequences

Kiplinger (1995) found two types of SHH behavior in HXBs: hardening peaks, HP, and hardening decays, HD (Section 2.2). To improve his SEP forecasting criteria he added the restriction that the SHH phase of the HP events should extend over peaks only with FWHM > 70 s. This restriction may be due to the fact that the energy spectral indices of HXB peaks are negatively correlated with their peak intensities, both for sub-peaks in a single flare and among different flares (Battaglia et al. 2005). A flare HXB sequence of progressively more intense bursts can therefore be expected to produce a composite SHH signature due to the increasingly harder burst spectra. A burst sequence lasting longer than the 70 s limit for a single HP event may therefore appear to satisfy the Kiplinger (1995) criteria even though each sub-burst manifests an SHS behavior. A candidate example (Figure 1 of Grayson et al. 2009) is the 2004 September 19 sequence of six bursts over about 8 minutes that results in an overall SHH signature. Another example is the decrease of γ from ~ 5 to 2 during the sequence of about five bursts over 5 minutes on 2004 November 10 (Figure 4). A third example is the four peaks during 0100–0105 UT on 2003 May 29 (Figure 5). Grayson et al. (2009) classify these example events as SHH, but do not state their relevant SHH periods.

Also instructive perhaps are the 2005 January 15 22:30 UT and January 19 events of Figure 3 of Saldanha et al. (2008). In the January 19 event a sequence of five bursts from 0812 to 0826 UT produces a significant decrease in γ , but the burst separations give a clear view of the individual SHS signatures, and Saldanha et al. (2008) do not consider that period to constitute SHH behavior. More ambiguous is the apparent SHH behavior from 2238 to 2244 UT of the January 15 22:30 UT flare, but that is also considered SHS by Saldanha et al. (2008). The point here is that classifying spectral behavior over a sequence of sub-bursts producing a combined SHH signature can be a subjective endeavor.

4.2. Background Effects on γ

A second source of confusion is that γ tends to decrease toward small values as the HXB fluxes decay to background. The *RHESSI* hard radiation background is not due to the quiet

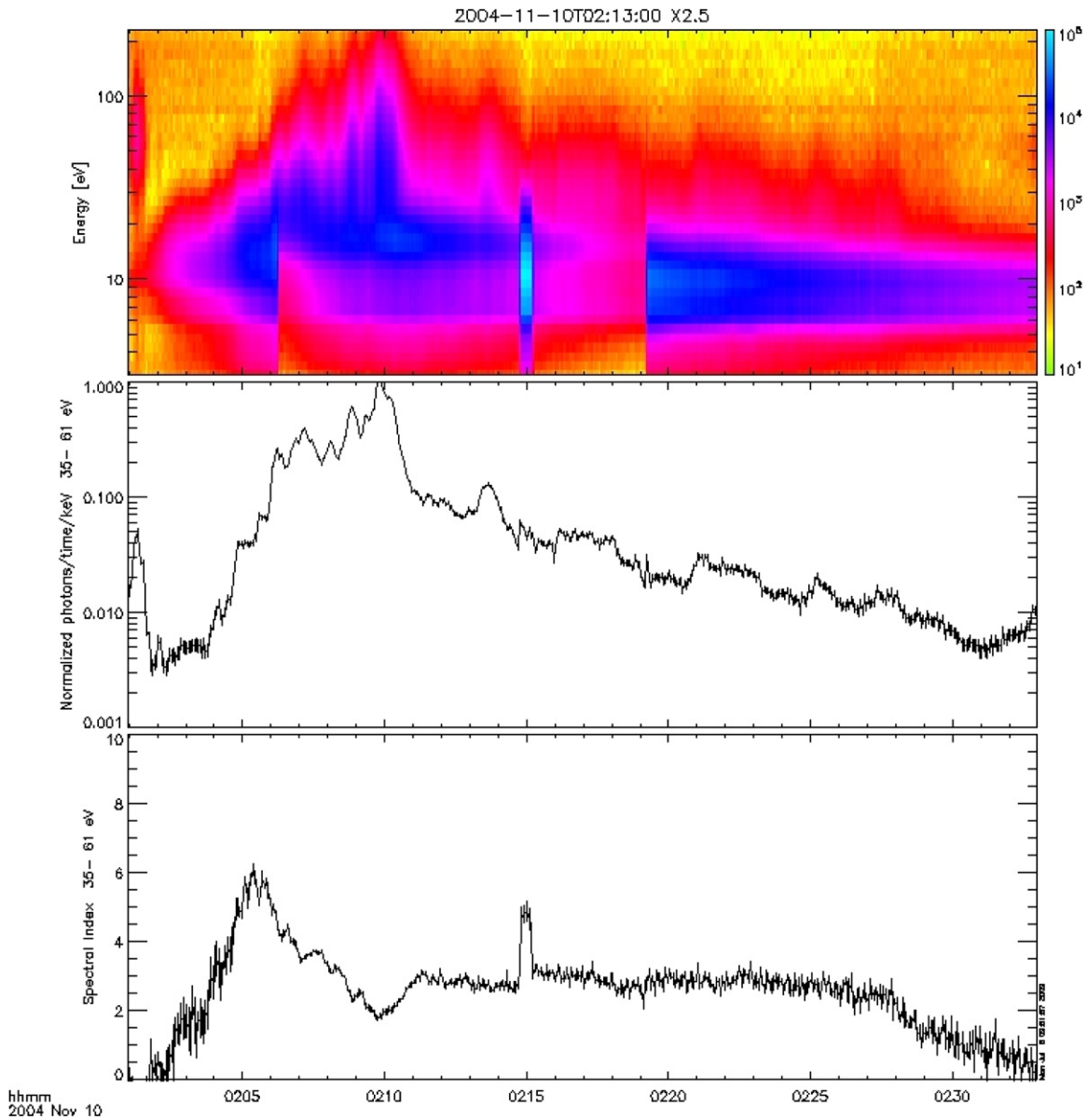


Figure 4. *RHESSI* dynamic plot of the 2004 November 10 SSH HXB. The top panel is a color-coded dynamic energy spectrum. The middle panel is the 35–61 keV flux plot, and the bottom panel is the spectral index γ over the time interval. The interval 0205–0210 UT is characterized by a succession of impulsive bursts which produce an SHH spectral behavior. From 0211 to 0227 UT γ is flat and then declines only as the X-ray burst flux approaches background.

(A color version of this figure is available in the online journal.)

Sun, for which only upper limits of the flux have been established (Hannah et al. 2010), but it is harder than solar flare spectra and can produce false SHH behavior (Grayson et al. 2009). A substantial flux decrease in the decay phase of a peak or in the late phase of a gradual decay could produce this behavior. As a check against this effect Grayson et al. (2009) calculated a signal-to-background (SB) ratio at the onset of SHH for each of the SHH events. Those SB ratios (Column 6 of their Table 1) range from ~ 5 to 36.

The only SHH behavior in the 2002 April 21 HXB (Figure 1 of Grayson et al. 2009) occurs 0215–0240 UT and is characterized by the low SB event ratio of 4.8. The SHH classification may be appropriate there, but the gradual decay of γ from ~ 2.5 to 1.5 and the low flux during that time suggest a background effect. A similar problem may be present in the Grayson et al. (2009) SHH HXBs of 2002 August 21, 2003 April 24, and 2003 May

29, the last of which is shown in Figure 5). We also note that in Figure 4 γ shows an SHS behavior through the sequence of bursts from 0206 to 0210 UT and is clearly SHH only after 0226 UT as the flux approaches background. A similar situation may characterize the 2005 January 19 HXB of Figure 3 of Saldanha et al. (2008). The period after 0108 UT of Figure 5 shows a clear effect of the background on γ . The background effect is mitigated by checking for appropriately high SB ratios, but it may still present a challenge in identifying SHH HXB signatures.

4.3. Energy Dependence and Definition of SHH

An energy dependence of γ is another potential pitfall for the SHH criterion. In the 100–200 keV range the 2005 January 20 HXB shows an SHH behavior through each peak (Figure 3 of Saldanha et al. 2008) but the 50–100 keV plot of γ used

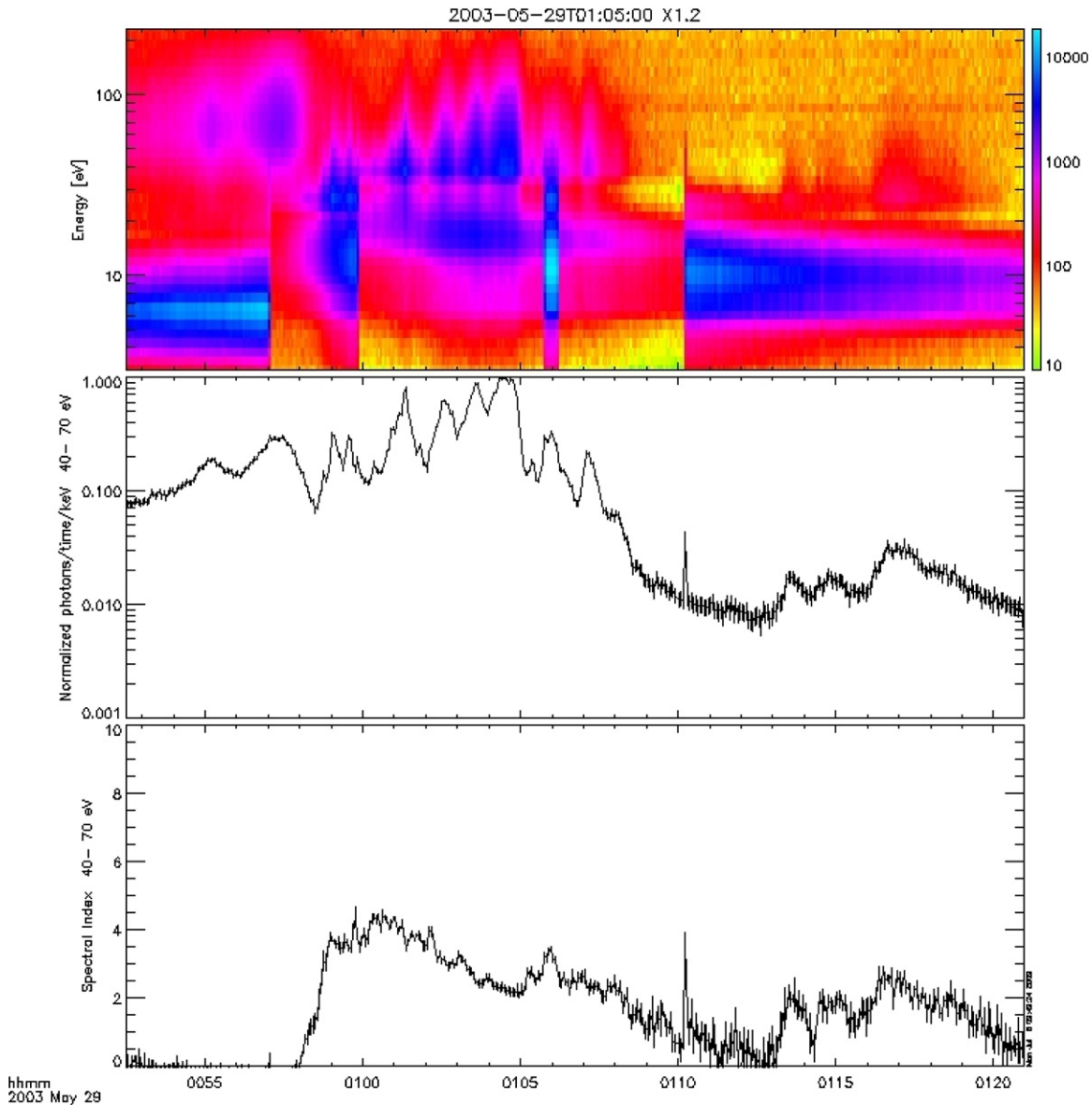


Figure 5. *RHESSI* dynamic plot of the 2003 May 29 SSH HXB. The top panel is a color-coded dynamic energy spectrum. The middle panel is the 40–70 keV flux plot, and the bottom panel is the spectral index γ over the time interval. The interval 0101–0105 UT is characterized by a succession of impulsive bursts which produce an SHH spectral behavior. After 0107 UT γ declines and correlates with the HXB flux, producing apparent HSH burst behavior due to the effect of the hard spectral background.

(A color version of this figure is available in the online journal.)

in the Grayson et al. (2009) analysis shows an SHS behavior superposed on a γ value of ~ 3 during the 0640–0652 UT peak. Thus, whether an HXB shows an SHH behavior can depend critically on the X-ray energy range examined.

A final concern is that the only SHH criterion for γ is that it must decline after a peak or in the gradual flux decay, but there is no quantitative requirement for that decline. Thus, whether the flat (e.g., from 0211 to 0226 UT in Figure 4) or very slowly changing (e.g., from 2258 to 2310 UT of 2005 January 15 at 2230 UT of Saldanha et al. (2008)) spectra are sufficiently hardening to be SHH HXBs are judgment tests of the viewer.

The HXB spectral ambiguities due to progressively more intense sequential bursts, background effects, and energy dependence outlined in this section do not invalidate the SHH criterion, but they need to be quantitatively addressed before a predictive tool for SEP events can be made.

5. DISCUSSION

5.1. Connecting SXR Flares, HXBs, and CMEs to SEP Events

The SHH HXBs may prove a useful tool for forecasting SEP events, but that does not imply that the SEPs observed in interplanetary space must originate in the same source regions as the HXBs. Our thesis is that the CME is the critical connection between SEP events and eruptive solar flares, whose HXBs are usually GHXBs characterized by SHH spectral behavior. We saw in Section 3 that ad hoc criteria based on the widths of the CMEs and durations of the SXR flares associated with the Grayson et al. (2009) *RHESSI* events could produce predictive results for SEP events matching those of the SHH criterion.

Statistical work with 69 *GOES* SXR flares by Kay et al. (2003) showed that SXR flares with associated CMEs were both cooler and longer in duration than those without CMEs.

With the understanding that CME shocks are required for SEP events, we can now understand the associations of SEP events with SXR flares of lower temperatures and longer durations found by Garcia (1994, 2004a) and Kubo & Akioka (2004). A consequence is that SXR flare fluence is now an SEP-event forecast tool (Balch 2008; Laurenza et al. 2009). A study of 15 *GOES* X-class SXR flares without accompanying CMEs by Klein et al. (2010) emphasizes the fact that intense SXR flares can be vigorous accelerators of microwave-emitting electrons but not produce interplanetary SEP events.

The success of the SHH criteria for forecasting SEP events suggests that GHXBs and SXR flares should have some connection to the process by which CMEs are accelerated. Impulsive acceleration of CMEs occurs during the maximum energy release in solar flares (e.g., Temmer et al. 2008, 2010), but in the post-impulsive phases Cheng et al. (2010) found that CME accelerations continued to be positive in SXR flares with long decay times, while deceleration was the rule in SXR flares with short decay times. This suggests that the continued energy release is shared between heating of the SXR flare region and the propulsion of the CME.

In three *RHESSI* flares extending to the 200–800 keV γ -ray range Krucker et al. (2008) observed that high coronal sources became prominent as the γ -ray emission decreased. Although they did not explicitly make the SHH connection, the longer timescales for higher energy electrons, harder spectra, and decreasing HXB fluxes were consistent with the characteristics found by Grigis & Benz (2008) in five SHH X-class flares, four of which were SHH events of either Grayson et al. (2009) or Saldanha et al. (2008). These HXR imaging results complemented the earlier study by Silva et al. (2000) of 57 HXR burst peaks in 27 flares with the BATSE instrument on the *Compton Gamma Ray Observatory*. They found SHH behavior to be much more likely in non-impulsive (duration > 2 minutes) bursts and in later, rather than earlier, peaks of events.

From these results a straightforward synthesis of the SHH XRBs emerges. Referring back to Figure 1, SEPs are produced in the shock driven by the CME. The flare impulsive phase takes place in the trailing reconnection region, producing the impulsive HXBs in the flare footpoints characterized by SHS behavior. During the subsequent gradual phase, the coronal source region, expanding and rising behind the fast CME becomes relatively brighter compared with the footpoint sources, and the combined signature becomes SHH as the HXB decays in intensity. Models indicate that both the SHS and SHH spectral behavior can result from turbulent stochastic acceleration in the reconnection current sheets of large loop structures under the CME (Bykov & Fleishman 2009).

5.2. Importance of Small Flares and Small SEP Events for the Kiplinger Effect

In Section 2.2, we pointed out that the reported success of the Kiplinger SHH prediction scheme derives largely from the many HXBs without associated SEP events. In particular, 188 of the 193 smaller (<5000 counts s^{-1}) and 136 of the 152 larger HXRBS HXBs of the Kiplinger (1995) study (parts B and C, Table 1) did not meet the SHH prediction criteria and were not associated with NOAA SEP events. From Table 4 of Kiplinger (1995) we see that the SXR flares involved in his larger HXB study that were either SHH events or associated with NOAA SEP events were predominately X-class with some larger M-class flares. Sizes of those HXB flares associated with neither SHH behavior nor NOAA SEP events were not given, but were

very likely smaller flares. Our success metric M_{scs} (the ratio of correct to incorrect SEP event predictions) excludes these numerous small flares which, based on SXR size alone, might be considered unlikely candidates for SEP event associations. M_{scs} was 4/1 for NOAA SEP events for the smaller HXBs of his study and 10/6 for the larger (parts B and C of Table 1). These numbers contrast with the strikingly high success rates for forecasting NOAA SEP events cited in Section 1.

A serious limitation of the previously cited HXB studies is that the inverse study beginning with all observed gradual SEP events has not been done. The first Kiplinger (1995) study dealt only with all SEP events associated with large HXRBS flares. His second study considered only NOAA SEP events with associated HXRBS HXBs sufficiently well observed to determine the presence of SHH spectral behavior. A study beginning with all SEP events, either of all intensities or only of NOAA class, independent of HXRBS HXB associations was not done. We can perhaps get some indication of what this limitation means from the validation study of the US Air Force Proton Prediction System (PPS) by Kahler et al. (2007). Starting with all $\geq M5$ *GOES* SXR flares with identified solar source regions and considering only NOAA SEP events, the PPS successfully predicted 18 events and had three missed events and 18 false predictions, for a success metric $M_{scs} = 18/21$. However, another 24 NOAA SEP events were not predicted, mainly because they were associated with smaller $\leq M5$ flares and not used in the study. A significant number of large, even $E > 500$ MeV relativistic (Cliver et al. 1983) SEP events are associated with flares with weak impulsive phases. Inclusion of those additional 24 missed SEP events degrades the PPS M_{scs} to an unimpressive value of 18/45.

If we expand the $E > 10$ MeV SEP events from the ≥ 10 pfu NOAA events to those of ≥ 0.1 pfu and assume a differential power-law distribution of peak SEP intensities with an exponent of -1.37 (Belov et al. 2005), then the $24 + 18 + 3 = 45$ NOAA SEP events of the Kahler et al. (2007) validation study would be increased by an additional $\sim 4.5 \times 45 = 202$ smaller SEP events. Further assuming that nine of those 18 false predictions of NOAA SEP events would appear as smaller SEP events, we would then get a PPS M_{scs} of $(18 + 9)/(3 + 9 + 193) = 27/205$, the ratio now heavily dominated by the missed SEP events. Since the SHH criterion is similarly based on large HXB flares with known locations, we can expect the SHH criterion to match the poor PPS results for predicting the > 0.1 pfu SEP events.

6. SUMMARY

For observed HXBs with sufficient intensity and duration the SHH criteria may be a good predictor of large SEP events. We argue here that the success of the SHH criteria is due not to a common acceleration of the SEPs along with the HXB energetic electron population, but rather to a common association in large eruptive flares of both CME-driven shocks and populations of energetic electrons accelerated in reconnecting coronal magnetic loops. Unlike the SEPs, which extend over many tens of degrees of open coronal and interplanetary magnetic fields after production in CME-driven shocks, the energetic electrons producing the HXBs populate high expanding coronal magnetic fields. It is therefore not surprising to find that other solar eruptive event signatures, such as lower temperatures or longer durations of SXR events or the broader widths of the associated CMEs, can produce comparable prediction statistics. This is a confirmation of the basic concept

of eruptive events discussed by Cliver et al. (1986) and illustrated in Figure 1.

The SHH signature is generally observed during the decay phase of a long-lived HXB and requires careful discrimination against apparent SHH signatures due to sequences of successively harder XRB pulses or to flux levels partially dependent on the hard spectral background. The lack of specific numerical requirements for the temporal decrease in γ and the possibility of energy-dependent SHH behavior are further areas that need to be clearly quantified and consistently applied in subsequent studies before a reliable SEP forecasting tool can be made based on SHH signatures.

There is also a large population of SEP events smaller than the NOAA SEP events which will not be predicted because of a lack of sufficiently large associated HXBs. These smaller ($F_p > 0.1$ pfu) SEP events have not been accounted for in previous SHH-SEP event association studies. We also point out that much of the apparent success of the SHH criteria is due to the large number of smaller non-SHH XRBs which are not associated with SEP events. We introduced a simple metric M_{scs} , the ratio of correct to incorrect (missed and false alarms) forecasts to characterize the SHH and flare/CME studies. Using only the HXB flares of the Grayson et al. (2009) study, we defined SXR flare duration and CME width criteria that produced M_{scs} values of 11/5 and 14/1, respectively, somewhat better than the Kiplinger (1995) and Grayson et al. (2009) values of 18/10 and 16/6 for SEP events of $F_p > 0.1$ pfu (Table 2).

This work was funded by AFOSR task 2301RDZ4. I thank G. Share and A. Tylka for useful discussions, the ApJ reviewer for substantial improvements in the paper, and James Grayson for posting plots of all the *RHESSI* dynamic spectra of the events of the Grayson et al. (2009) study on his Web site. This work made use of the LASCO CME catalog, which is generated and maintained at the CDAW Data Center by NASA and The Catholic University of America in cooperation with the Naval Research Laboratory. *SOHO* is a project of international cooperation between ESA and NASA.

REFERENCES

- Aschwanden, M. J. 2012, *Space Sci. Rev.*, in press
- Balch, C. C. 2008, *Space Weather*, 6, S01001
- Battaglia, M., Grigis, P. C., & Benz, A. O. 2005, *A&A*, 439, 737
- Belov, A., Garcia, H., Kurt, V., Mavromichalaki, H., & Gerontidou, M. 2005, *Sol. Phys.*, 229, 135
- Bykov, A. M., & Fleishman, G. D. 2009, *ApJ*, 692, L45
- Cane, H. V., Mewaldt, R. A., Cohen, C. M. S., & von Rosenvinge, T. T. 2006, *J. Geophys. Res.*, 111, A06S90
- Cane, H. V., Richardson, I. G., & von Rosenvinge, T. T. 2010, *J. Geophys. Res.*, 115, A08101
- Cheng, X., Zhang, J., Ding, M. D., & Poomvises, W. 2010, *ApJ*, 712, 752
- Cliver, E. W. 2009, in IAU Proc. 257, *Universal Heliospheric Processes*, ed. N. Gopalswamy & D. F. Webb (Cambridge: Cambridge Univ. Press), 401
- Cliver, E. W., Dennis, B. R., Kiplinger, A. L., et al. 1986, *ApJ*, 305, 920
- Cliver, E. W., Kahler, S. W., Cane, H. V., et al. 1983, *Sol. Phys.*, 89, 181
- Dennis, B. R. 1988, *Sol. Phys.*, 118, 49
- Firoz, K. A., Moon, Y.-J., Cho, K.-S., et al. 2011, *J. Geophys. Res.*, 116, A04101
- Garcia, H. A. 1994, *ApJ*, 420, 422
- Garcia, H. A. 2004a, *Space Weather*, 2, S02002
- Garcia, H. A. 2004b, *Space Weather*, 2, S06003
- Garcia, H. A., & McIntosh, P. S. 1992, *Sol. Phys.*, 141, 109
- Gopalswamy, N., Akiyama, S., & Yashiro, S. 2009, in IAU Proc. 257, *Universal Heliospheric Processes*, ed. N. Gopalswamy & D. F. Webb (Cambridge: Cambridge Univ. Press), 283
- Gopalswamy, N., Xie, H., Yashiro, S., & Usoskin, I. 2005, in Proc. 29th ICRC, Vol. 1, 169
- Gopalswamy, N., Yashiro, S., Kaiser, M. L., Howard, R. A., & Bougeret, J.-L. 2001, *J. Geophys. Res.*, 106, 29219
- Gopalswamy, N., Yashiro, S., Xie, H., et al. 2008, *ApJ*, 674, 560
- Grayson, J. A., Krucker, S., & Lin, R. P. 2009, *ApJ*, 707, 1588
- Grechnev, V. V., Kurt, V. G., Chertok, I. M., et al. 2008, *Sol. Phys.*, 252, 149
- Grigis, P. C., & Benz, A. O. 2008, *ApJ*, 683, 1180
- Hannah, I. G., Hudson, H. S., Hurford, G. J., & Lin, R. P. 2010, *ApJ*, 724, 487
- Hudson, H. S. 2011, *Space Sci. Rev.*, 158, 5
- Kahler, S. W. 2005, *ApJ*, 628, 1014
- Kahler, S. W., Cliver, E. W., & Ling, A. G. 2007, *J. Atmos. Solar Terr. Phys.*, 69, 43
- Kahler, S. W., & Reames, D. V. 2003, *ApJ*, 584, 1063
- Kay, H. R. M., Culhane, J. L., Harra, L. K., & Matthews, S. A. 2003, *Adv. Space Res.*, 32, 1051
- Kiplinger, A. L. 1995, *ApJ*, 453, 973
- Klein, K.-L., Trottet, G., & Klassen, A. 2010, *Sol. Phys.*, 263, 185
- Kocharov, L., Cho, K.-S., & Valtonen, E. 2011, *ApJ*, 735, 4
- Kocharov, L., Reiner, M. J., Klassen, A., Thompson, B. J., & Valtonen, E. 2010, *ApJ*, 725, 2262
- Kosugi, T., Dennis, B. R., & Kai, K. 1988, *ApJ*, 324, 1118
- Krucker, S., Hurford, G. J., MacKinnon, A. L., Shih, A. Y., & Lin, R. P. 2008, *ApJ*, 678, L63
- Kubo, Y., & Akioka, M. 2004, *Space Weather*, 2, S01002
- Kuznetsov, S. N., Kurt, V. G., Yushkov, B. Yu., & Kudela, K. 2008, in Proc. 30th ICRC, Vol. 1, 121
- Laurenza, M., Cliver, E. W., Hewitt, J., et al. 2009, *Space Weather*, 7, S04008
- Masson, S., Klein, K.-L., Butikofer, R., et al. 2009, *Sol. Phys.*, 257, 305
- McCracken, K. G., Moraal, H., & Stoker, P. H. 2008, *J. Geophys. Res.*, 113, A12101
- Michalek, G., Gopalswamy, N., & Xie, H. 2007, *Sol. Phys.*, 246, 409
- Miroshnichenko, L. I., Vashenyuk, E. V., Balabin, Yu. V., Perez-Peraza, J., & Gvozdevsky, B. B. 2009, in Proc. 31st ICRC, <http://icrc2009.uni.lodz.pl/proc/pdf/icrc1171.pdf>
- Nonnast, J. H., Armstrong, T. P., & Kohl, J. W. 1982, *J. Geophys. Res.*, 87, 4327
- Perez-Peraza, J., Vashenyuk, E. V., Miroshnichenko, L. I., Balabin, Yu. V., & Gallegos-Cruz, A. 2009, *ApJ*, 695, 865
- Reames, D. V. 1999, *Space Sci. Res.*, 90, 413
- Saldanha, R., Krucker, S., & Lin, R. P. 2008, *ApJ*, 673, 1169
- Silva, A. V. R., Wang, H., & Gary, D. E. 2000, *ApJ*, 545, 1116
- Simnett, G. M. 2006, *A&A*, 445, 715
- Temmer, M., Veronig, A. M., Kontar, E. P., Krucker, S., & Vrsnak, B. 2010, *ApJ*, 712, 1410
- Temmer, M., Veronig, A. M., Vrsnak, B., et al. 2008, *ApJ*, 673, L95
- Vashenyuk, E. V., Balabin, Yu. V., & Gvozdevsky, B. B. 2009, in Proc. 31st ICRC, <http://icrc2009.uni.lodz.pl/proc/pdf/icrc1304.pdf>
- Yashiro, S., & Gopalswamy, N. 2008, in IAU Proc. 257, *Universal Heliospheric Processes*, ed. N. Gopalswamy & D. F. Webb (Cambridge: Cambridge Univ. Press), 233
- Yashiro, S., Gopalswamy, N., Akiyama, S., Michalek, G., & Howard, R. A. 2005, *J. Geophys. Res.*, 110, A12S05